Journal of Applied Electrochemistry (2007) 37:405–413
DOI 10.1007/s10800-006-9271-3

Stability of spontaneous passive films on high strength Mo-containing stainless steels in aqueous solutions

F. EL-TAIB HEAKAL*, A.A. GHONEIM and A.M. FEKRY
Chemistry Department, Faculty of Science, Cairo University, Giza, Egypt
*(*author for correspondence, e-mail: fakihaheakal@yahoo.com)*

Received 17 October 2005; accepted in revised form 18 October 2006

Key words: chloride, CPE, EIS, Mo-containing steels, passive films, pH, spontaneous growth, sulphate

Abstract

The stability of naturally grown passive films on some Mo-containing stainless steel specimens was examined in aerated and deaerated universal buffer solutions with different pH (2–12) as well as in sulphate and chloride solutions. Open circuit potential (E_{oc}) and electrochemical impedance spectroscopy (EIS) were used as measuring techniques. In all cases, E_{oc} shifts towards less negative values with time until the potential reaches its steady-state (E_{ss}) value. The E_{ss} value is found to be more positive with decrease in solution pH or increase in Mo content in the alloy and becomes less positive in deaerated buffer solutions. Also, the thickening rate of the outer layer for the duplex passive film increases with increasing extent of Mo in the steel substrate or pH of the test solution. For a given alloy, E_{ss} decreases linearly with the anion concentration (C), and is always more positive in Cl^- than in SO_4^{2-} media for $C \geq 0.05$ M. Analysis of the EIS data showed that the total resistance (R_T) of the passive film has higher values in aerated solutions, and is generally lower in basic solutions. This indicates that lower solution pH favours the formation of oxide films offering better protection. Furthermore, the higher values of R_T in Na_2SO_4 solutions suggest the formation of more stable passive films in sulphate than in chloride solutions. This is discussed on the basis of the relative degree of anion incorporation into the passive films.

1. Introduction

Addition of Mo to the Cr–Ni stainless steels has long been known to improve their properties in many respects [1–5]. These include, diminishing the risk of passive film breakdown, especially in chloride-containing media and increasing both the passive film thickness and the alloy resistance for pitting and crevice corrosion. As for the stress corrosion cracking resistance of the alloys, Mo additions have shown variable effects [6], being detrimental with small additions of Mo and beneficial for alloy containing more than 4 wt%. It seems that Mo in some way helps the chromium present in a stainless steel to form the necessary passive films [7, 8], or prevents depassivation develop within crevices [9, 10].

The present work is devoted to investigate some of the factors that influence the electrochemical reactivity and stability of some stainless steel specimens containing various levels of Mo in aqueous solutions of different nature. The test solutions were extended to include universal buffers with pH range 2–12 in the presence or absence of naturally oxygen, as well as aerated chloride and sulphate solutions of various concentrations. Open circuit potential measurements and electrochemical impedance spectroscopy (EIS) were used.

2. Experimental details

Seven types of commercial Mo-containing stainless steels were supplied by Outokumpu Stainless in the form of plates (Table 1). The workpieces were prepared from the as-casted rectangular specimens and fixed to glass with a resin to project a cross-sectional area of 0.160 cm^2. The electrodes were mechanically polished with metallurgical papers and then rinsed with distilled water. Electrolytes were all prepared from analytical grade reagents and triply distilled water. A series of universal buffers (pH range 2–12) with constant ionic strength was prepared (100 ml of mixed acids: 0.04 M phosphoric, 0.04 M acetic acid and 0.04 M boric acid adjusted to the required pH by 0.2 M NaOH solution) [11].

The potentials were measured versus the saturated calomel electrode (SCE). Impedance measurements were performed in the frequency domain from 0.1 Hz to 100 kHz using an electrochemical workstation (IM6e Zahner electrik GmbH, Meßtechnik, Germany). The excitation ac signal had an amplitude of 10 mV peak to peak. All experiments were carried out at 298 K in naturally aerated solutions. Some tests were conducted in nitrogen saturated solutions, where purified N_2 gas

Table 1. Designation and chemical composition (in wt%) of the steels*

Steel No.	Designation	C	Cr	Ni	Mo	N	Others
I	SAF 2304	0.024	22.4	5.6	0.3	0.097	–
II	17–12-2.5	0.046	16.8	10.7	2.7	0.052	–
III	2205	0.019	21.9	5.7	3.0	0.148	–
IV	904 L	0.012	19.5	24.2	4.3	0.056	Cu 1.4
V	17-14-4 LN (or 317 L)	0.022	17.3	13.3	4.4	0.150	–
VI	254 SMO	0.017	19.7	17.9	6.0	0.195	Cu 0.7
VII	654 SMO	0.020	23.9	22.2	7.0	0.452	Cu 0.4, Mn 2.0

*The balance is the wt% of Fe in each steel.

was bubbled in the test solution for 20 min before each experiment and a flow of nitrogen was established above the solution during the measurements.

3. Results and discussion

3.1. *Behaviour in buffer solutions*

The open circuit potential (E_{oc}) of the steels containing varying amounts of Mo (0.3–7.0 wt%) was monitored over a period of 180 min until a steady state potential (E_{ss}) was reached. The test electrolytes were naturally aerated (NA-) and nitrogen saturated (N_2 sat-) universal buffer solutions of pH (2–12). The open circuit transients measured for the different steels have similar trends, where E_{oc} from the instant of immersion shifts with time in the positive direction, indicating a spontaneous passivation due to development of an oxide film [12]. This continues as a result of the predominance of the cathodic processes over the anodic ones until the film acquires a stable thickness. The necessary electrons of the cathodic reaction are provided by the ionization of metal atoms (most probably Cr atoms) entering the oxide phase. The results show that the stability of the steel surfaces is pH-dependent and increases greatly with decreasing solution pH and increasing Mo content in the alloy. Some of these results are given in Figure 1(a, b) as typical examples. Furthermore, the behaviour of steel I at pH 2 shown in Figure 1(c) shows that E_{ss} decreases as O_2 is replaced by N_2 in the test solution. E_{ss} also shows a clear dependence on Mo level in the alloy, where it increases, especially in the acidic and neutral buffer solutions, as the wt% Mo increases (Figure 2).

The E_{ss} value represents the free corrosion potential (E_{corr}) of the alloy under given experimental conditions. Figure 3(a) shows the dependence of E_{corr} on solution pH in NA-buffer solutions revealing that E_{corr} for alloys I–VII is a linear function of pH following the Nernstian form

$$E_{corr} = E^{o}_{corr} - \frac{2.3\,RT}{zF}\,\mathrm{pH} \qquad (1)$$

where E^{o}_{corr} is the corrosion potential at pH = 0 ($[H^+]$ = unity). The deviation of z from the expected value for the protolytic reaction at the interface with one electron transfer process may be related to a multistep

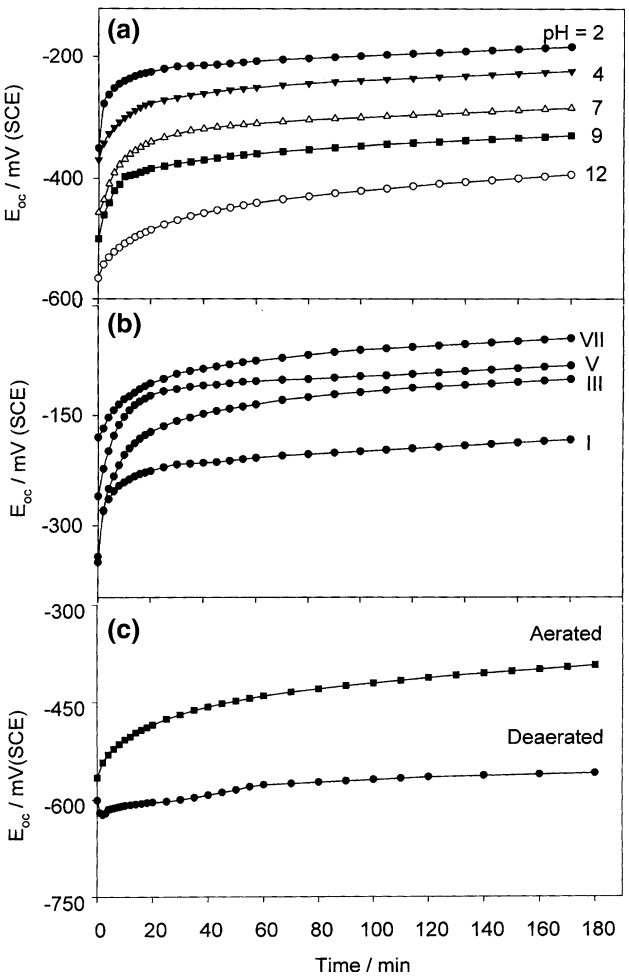

Fig. 1. Variation with time of the open circuit potential (E_{oc}) for: (a) steel I in NA-buffer solutions at various pHs; (b) steels I, III, V and VII in NA-buffer solution at pH 2; (c) steel I in NA- and in N_2 sat-buffer solution at pH 2.

film formation process. The slopes are found to range between −20 and −30 mV/pH, suggesting that passive film formation in aqueous buffer solutions is a two- or three- electron transfer process which can be represented as

$$\mathrm{Me} + z/2\ \mathrm{H_2O} \rightarrow \mathrm{MeO}_{z/2} + z\mathrm{H^+} + ze \qquad (2)$$

The anodic current may be supplied from an outer circuit or is compensated by cathodic current such as hydrogen or oxygen reduction at open circuit. On the

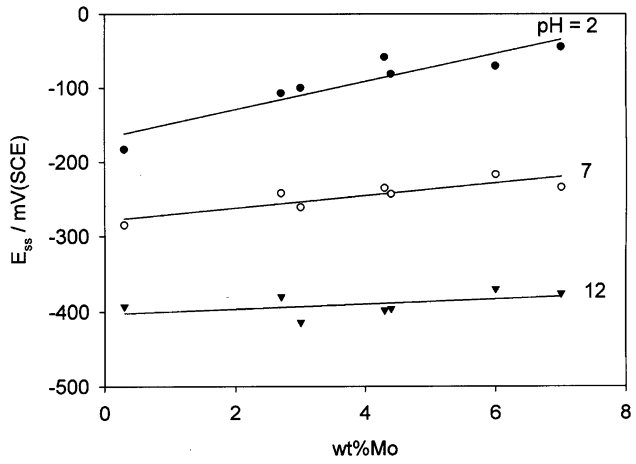

Fig. 2. Dependence of the steady state potential (E_{ss}) on Mo content of the steels in acidic (pH 2), neutral (pH 7) and alkaline (pH 12) NA- buffer solutions.

other hand, in N_2 sat- solutions there is a critical pH around a value of 9 after which E_{ss} increases with pH, as depicted in Figure 3(b) indicating a change in the sign and value of the slope in equation (1). This can be attributed to the interaction of both H^+ and OH^- ions with the electrode surface that is essentially covered with a passive film, or that the metal is oxidized by water molecules to form a stable oxide film.

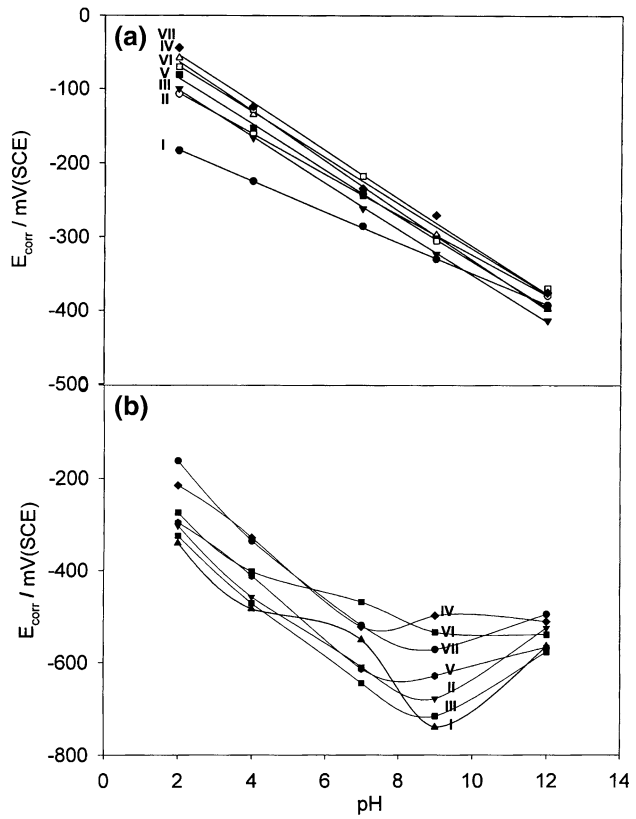

Fig. 3. (a) Free corrosion potential (E_{corr}) (after 180 min immersion) vs. pH for steels I–VII in NA-buffer solutions. (b) Free corrosion potential (E_{corr}) (after 180 min immersion) vs. pH for steels I–VII in N_2 sat-buffer solutions.

3.2. *Kinetics of oxide growth*

Real oxide films are usually non-stoichiometric due to an excess of metal cations or deficient oxygen anions. Oxide films with low electronic conductivity grow by ion migration and diffusion. Macdonald and Sun [13] used the point defect model (PDM) to derive the steady-state barrier layer thickness and passive current as a function of voltage. These are found to be consistent with the electronic character in both the passive and transpassive states. The impedance of the passive state is calculated as a function of the standard rate constants for the defect generation and annihilation reactions at the interface. The rate of barrier layer dissolution is found to have a major impact on the interfacial impedance and hence corrosion resistance. On the other hand, Bojinov et al used the mixed conduction model (MCM) to describe quantitatively the catalytic effect of Mo addition on the transpassive dissolution rate of the Fe–Cr [14] and of highly alloyed austenitic stainless steels [4]. The impedance spectra of the studied materials in the transpassive potential region were found to be consistent with the proposed kinetic model.

Under open circuit conditions, however, it is assumed that the oxide film grows via a solid state mechanism by the influence of a sufficiently high electric field strength to cause ionic migration and hence sustain self-diffusion of metal ions through semiconducting oxide films. Based on this notion a relationship between E_{oc} and immersion time (t) has been theorized as

$$E_{oc} = \text{constant} + 2.303\ (\delta/B)\ \log\ t \qquad (3)$$

in which δ is the rate of film thickening per decade of time and $B = (zF/RT)\alpha\kappa$, α being the transfer coefficient and κ the width of the energy barrier traversed by the metal ion during oxide formation [15]. Figure 4(a, b) shows the applicability of equation (3) to the present results for some tested steels as examples in NA- and N_2 sat- buffer solution of pH 2, respectively. The fact that equation (3) describes the behaviour of the various steels at initial as well as at later times indicates that oxide film growth follows a direct logarithmic law. The graphs shown in Figure 4(a, b) and the other similar plots consist of two straight segments. The change in the slope of each linear relationship is consistent with the duplex nature of the passive films. This is in agreement with the findings from surface analysis methods [16] showing that the passive film formed on austenitic stainless steel consists of an inner barrier layer of Fe–Cr- rich oxide and an outer hydroxide layer where Mo, if present in the alloy, is slightly enriched in the film. This outermost film existing in equilibrium with the electrolyte is evidently the one that determines the corrosion behaviour of the steel in aqueous solutions.

The rate of thickening δ_1 and δ_2 for the tested steels were calculated from the slopes of the straight lines in Figure 4(a, b) and similar plots, where δ_1 and δ_2 refer to the growth rate for the inner and outer passive layers, respectively. Results of these calculations for the

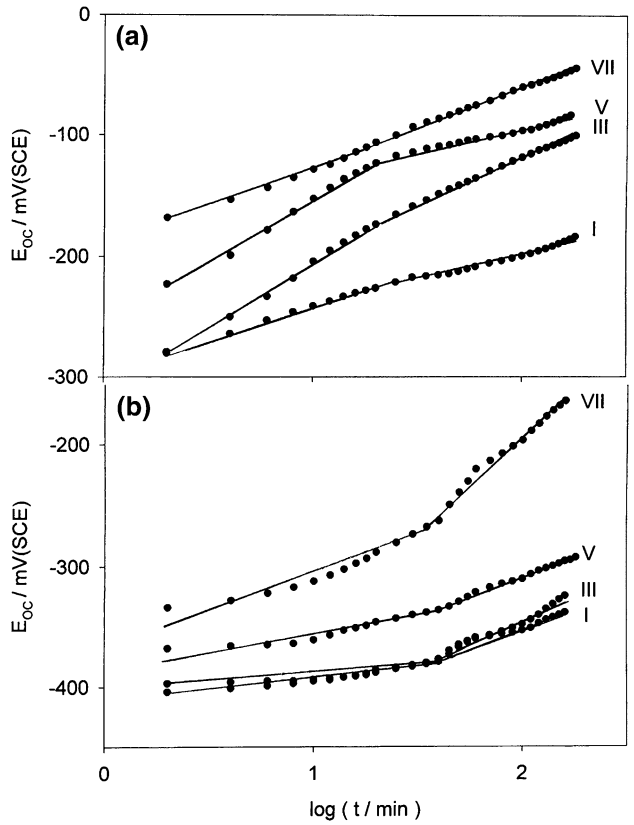

Fig. 4. E_{oc}-log time curves for steels I, III, V and VII at pH 2 in: (a) NA-buffer solution; (b) N_2 sat-buffer solution.

seven tested steels are given in Table 2 as a function of pH. In these calculations the value of α was taken as 0.5, that of κ as 1 nm [17] and an average value of 3 was computed for z, where the effect of large concentration of lower valent Ni ($z = 2$) is compensated by the smaller Mo content with higher valence ($z = 6$) [18]. It is clear from Table 2 that the values of δ_1 and δ_2 exhibit different dependence on pH, and that Mo plays an important role during the spontaneous growth of passive films on the steel surfaces. This can be made more obvious by comparing the variation with pH of δ_2 for the two steels I and III, having different Mo content while the other minor alloying elements are kept almost at the same level, as shown in Figure 5(a). The main feature of these results is that δ_2 is higher at any pH value for steel III as compared to steel I, and that the increase in pH of the test solution leads to an increase in δ_2, especially in highly alkaline buffer solution (pH 12). It can thus be concluded that increasing Mo level in the steel seems to sustain the formation of thicker outermost passive layers [3, 5], which is aided by pH increase of the test solution. Another feature is that δ_2 is related exponentially with pH as substantiated from the uncertainty estimate shown in Figure 5(b). Perhaps the oscillations in the results of steel I are due to the low Mo content (0.3 wt %) in this alloy.

3.3. *Influence of SO_4^{2-} and Cl^- anions*

The effect of solution nature and concentration on the corrosion behaviour of three steels (III, V and VII) was also studied. Figure 6(a, b) shows a typical example for the potential behaviour of steel III in aerated Na_2SO_4 and NaCl solutions, respectively. As shown by this figure, and the similar ones for steels V and VII, in most of the studied concentrations, the potential tends at first towards more negative values assuming instability of the pre-immersion passive film. However, after a certain time, slightly dependent on solution and alloy composition, the potential changes positively with time [19], indicating healing and further thickening until attaining the E_{ss} values which become less noble with increasing anion concentration (C). As shown in Figure 6(c), the linear variation of E_{ss} with log C follows the relation

$$E_{ss} = y - m \log C \quad (4)$$

where y is the E_{ss} value in solution of unit concentration and the slope m is dependent on the corroding surface and the corrosiveness of the medium. The shift of E_{ss} toward negative values indicates a more facile film dissolution reaction whose rate exceeds that of film repair with increasing anion concentration. The degree of this shift (i.e. m value) estimated for steel III, ranges between 12 mV/decade in Cl^- and 39 mV/decade in

Table 2. Thickening rates δ_1 and δ_2 (in nm/decade) for the inner and outer layers of the passive films on steels I–VII in both NA- and N_2 sat- buffer solutions of different pH

pH	Thickening rate/nm decade^{-1}	NA-Solutions							N_2 Sat-Solutions						
		Steel No.													
		I	II	III	IV	V	VI	VII	I	II	III	IV	V	VI	VII
2	δ_1	1.41	2.66	2.73	2.23	2.63	2.46	1.45	0.19	0.6	0.49	0.88	0.45	0.81	1.3
	δ_2	1.02	0.92	2.15	1.15	1.3	1.38	1.75	1.24	1.38	1.6	2.39	1.32	2.41	3.3
4	δ_1	1.49	2.5	2.04	1.72	2.89	2.09	2.26	0.62	0.4	0.4	1.03	0.57	0.65	0.55
	δ_2	1.79	1.8	2.09	1.87	1.99	1.63	1.8	0.84	0.86	0.85	1.53	1.28	1.7	3.3
7	δ_1	2.44	1.89	1.87	1.88	1.42	1.58	1.09	0.35	0.55	0.41	–	0.17	1.31	0.7
	δ_2	1.71	2.15	2.15	1.3	1.61	1.48	1.62	1.58	0.48	0.51	–	0.18	1.86	0.76
9	δ_1	2.3	1.62	1.42	1.49	0.82	1.02	1.79	–	–	–	0.24	0.46	–	–
	δ_2	1.31	1.71	2.21	1.66	1.44	1.14	1.61	0.76	1.21	1.33	0.9	1.89	4.5	4.09
12	δ_1	1.33	1.23	1.92	1.15	1.54	2.77	3.08	–	0.69	1.69	0.92	1.46	–	1.85
	δ_2	2.38	2.77	2.69	2.69	2.69	1.69	1.69	–	2.61	1.92	1.77	3.84	–	2.46

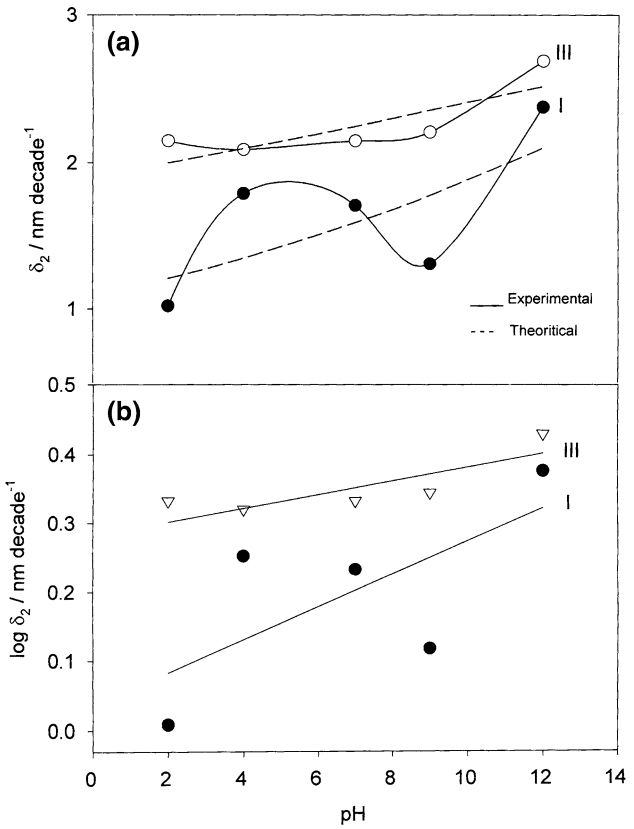

Fig. 5. Variation with pH of: (a) mean oxide thickening rates of the outer passive layer δ_2 for steels I and III; (b) Experimental and theoretical δ_2 values on a semilog plot for steels I and III in NA- buffer solutions (correlation coefficient: $r^2_{\mathrm{I}} = 0.47$ and $r^2_{\mathrm{III}} = 0.65$).

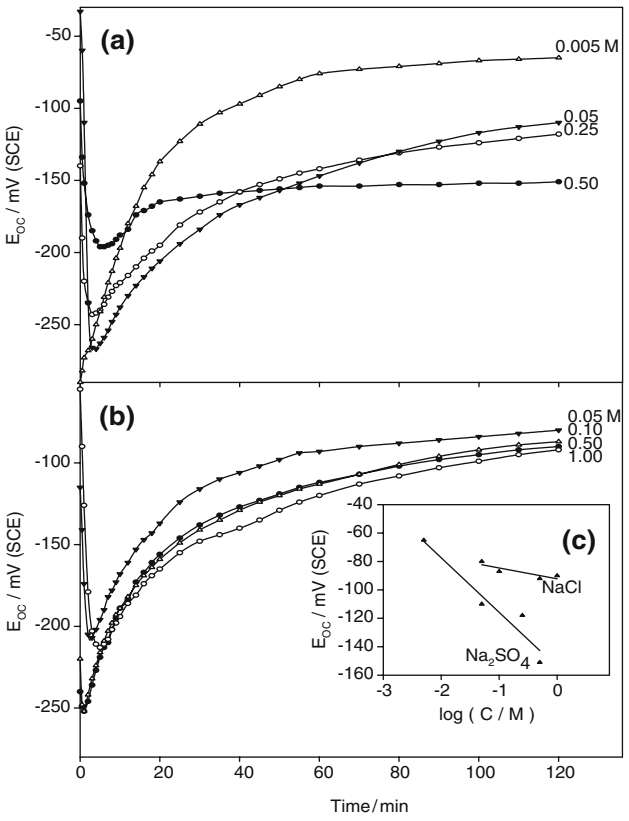

Fig. 6. Variation with time of the open circuit (E_{oc}) as a function of concentration for steel III in: (a) Na_2SO_4 solutions; (b) NaCl solutions. (c) E_{ss}-log C dependence in Na_2SO_4 and NaCl solutions.

SO_4^{2-}. Nevertheless, these values are still around those characteristic of oxide/solution interface reactions but with a different number of electrons exchanging at the interface [15]. Also, E_{ss} value for any steel is found to be more positive in chloride than in sulphate medium with the same concentration (≥0.05 M). It has been suggested that when the passive film is grown in a Cl^- containing electrolyte, Mo forms not only insoluble chlorides, but also soluble oxochlorocomplexes [20]. Thus less Cl^- will be built into the passive film during its formation and growth. Consequently, in the presence of Mo, the steel becomes more resistant to corrosive attack and the free corrosion potential or E_{ss} value of the alloy is increased. In addition, the difference between the solubility and concentration of oxygen in the two media may also contribute to the higher E_{ss} values in Cl^- than in SO_4^{2-} solutions.

This behaviour can be further explained by comparing the variation of the outer layer thickening rate (δ_2) for steel III with log C as shown in Figure 7. In Na_2SO_4 solutions δ_2 shows a marked dependence on concentration, where it decreases sharply and linearly with log C, while in NaCl solutions δ_2 first decreases passing a minimum value at ~0.1 M, then it starts to increase with concentration. The different dependence of δ_2 on the Cl^- and SO_4^{2-} ions concentration may be related to the difference in the corrosiveness of the two media towards the alloy passive film leading to different modes of corrosion attack, pitting in the former and general in the later.

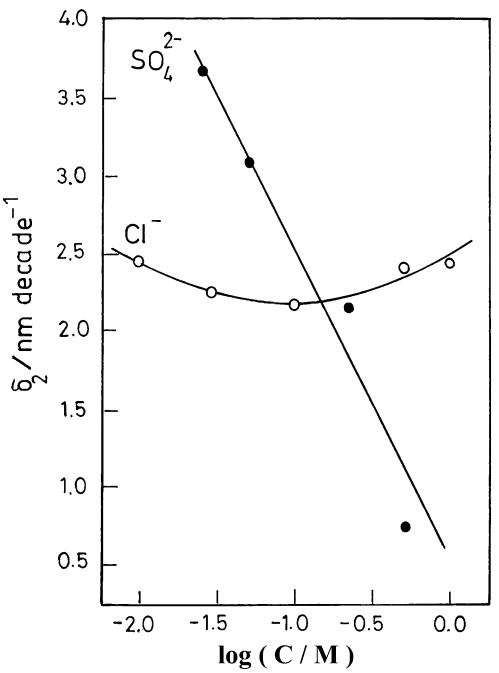

Fig. 7. Variation of the outer layer thickening rate (δ_2) for steel III with log C in Na_2SO_4 and NaCl solutions.

3.4. *EIS measurements*

To obtain further confirmation for the relative stability of spontaneous passive films on the various steels, impedance spectra were recorded at E_{corr} (after 3 h of electrode immersion). Figure 8(a) shows a typical example of impedance spectra as Bode plots for steel I in NA-buffers (pH 2, 7 and 12). The corresponding plots in N_2 sat- solutions are also given in Figure 8(b). The Bode plots are all characterized by a capacitive contribution only at intermediate frequencies, which corresponds to a maximum in the phase angle θ vs. log *f*. Although the electrochemical impedance was measured down to very low frequencies (100 mHz), the Bode plots do not show a resistive region (horizontal line and a phase angle $\theta \sim 0$ °) at these frequencies. This is in agreement with previous work by Kim [21], indicating that no second time constant can be discerned under any test conditions. Using a constant phase element (CPE), the simple Randles equivalent circuit displayed in Figure 8(c) was found to be satisfactory for fitting the impedance data. The CPE is defined in the impedance forms as [22]

$$Z_{CPE} = [Q(j\omega)^{\alpha}]^{1} \quad (5)$$

where α is associated with the roughness of the electrode surface and has a value between 0.5 (for a porous electrode) and unity (for ideally flat electrode), *j* is $\sqrt{-1}$, ω is angular frequency ($\omega = 2\pi f$ rad s^{-1}) and *Q* is a frequency-independent real constant representing the total capacitance of the CPE and having units of F s^{α} (i.e. Ω^{-1} s^{α}). The theoretical simulated impedance parameters for the seven tested Mo-bearing stainless steel electrodes in universal buffer solutions of pH 2, 7 and 12 are summarized in Table (4) for the naturally oxygenated solutions as well as the N_2-saturated ones. The results show clearly that the capacitance of the passive film on any steel surface acquires higher values with decreasing pH or by purging the solution with N_2 gas. Assuming that the Q value is a summation of more than one series capacitances, namely the double layer C_D and the passive film C_P, then

$$Q^{-1} = C_D^{-1} + C_P^{-1} \quad (6)$$

when C_D is much greater than C_P, then $Q \sim C_P$, which is given by the simple relation

$$C_P = \varepsilon_r \varepsilon_r^o / \delta \quad (7)$$

where ε_r^o is the permittivity of free space (8.85×10^{-12} F m^{-1}), ε_r is the dielectric constant of the passive film and δ (in cm) is the passive film thickness. The results for *Q* show, in general, that there is a possible tendency for hydration of the passive film to various degrees, depending on pH of the forming solution, irrespective of the alloy composition. Thus, a film grown in solution of higher pH has lower *Q* value due to the lower dielectric constant (ε_r) of the film as a result of the extensive hydration. On the other hand, deareation of the solutions by N_2 gas decreases this tendency leading to somewhat higher *Q* values compared to those in oxygenated solutions. In this respect, it is necessary to indicate that the tendency for hydration with increasing pH of the forming solutions coincides with the observed systematic decrease in E_{ss} values.

The degree of passivation and stability of the surface films is best explained by considering the values of R_T, estimating the total resistance of the oxide film [21]. As a general trend, Table 3 shows that R_T values tend to be lower in alkaline than in the acidic solutions and fall in the MΩ and kΩ ranges in the presence and absence of air oxygen, respectively. This behaviour indicates that the passive film is liable to dissolve in caustic solutions more than in acid ones, showing that the formation-dissolution process of the oxide film is shifted more towards

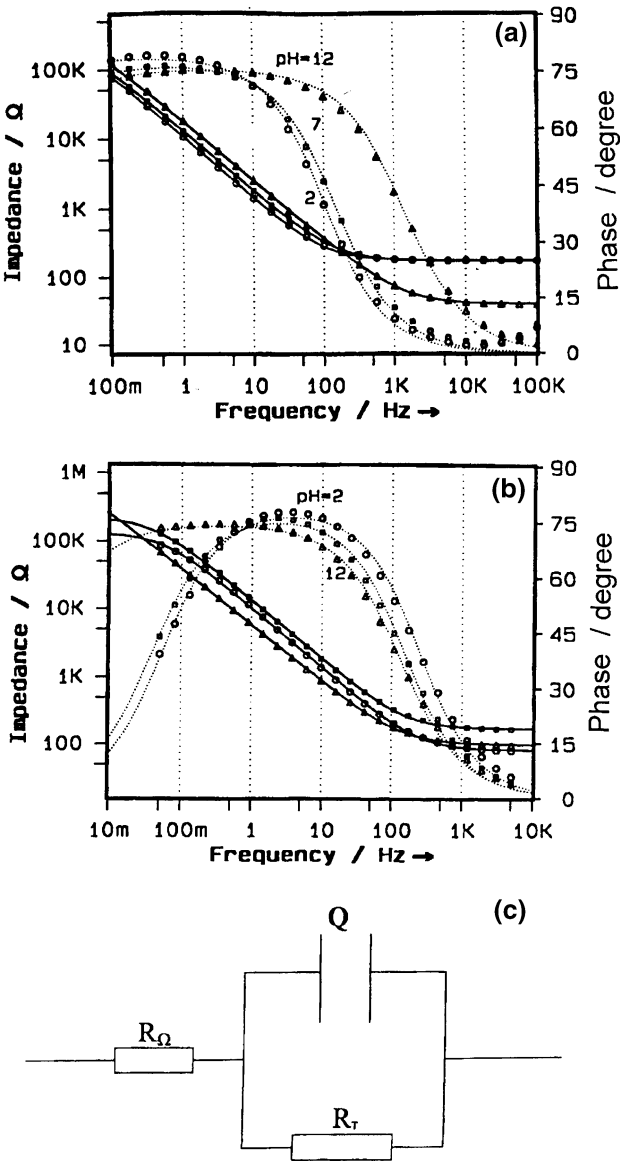

Fig. 8. EIS Bode plots for steel I in buffers of pH 2, 7 and 12; (a) NA-solutions; (b) N_2 sat-solutions. (□, ○, △) experimental data; and (...) theoretical data. (c) Equivalent circuit model representing the electrode/passive film/electrolyte system.

Table 3. Equivalent circuit parameters for steels I–VII in both NA- and N_2 sat-buffer solutions of pH 2, 7 and 12

Electrode No.	pH	(NA-Solutions)				(N_2 Sat-Solutions)			
		R_Ω/Ω	Q /μF	R_T/MΩ	α	R_Ω/Ω	Q /μF	R_Ω/Ω	α
I	2	145.8	5.95	3.5	0.888	81.0	5.93	228.7	0.861
II		156.9	7.24	3.1	0.860	84.2	5.73	270.7	0.789
III		148.0	6.74	2.7	0.872	79.2	5.63	229.8	0.826
IV		177.4	6.37	5.7	0.874	82.3	7.11	381.9	0.866
V		142.8	7.06	4.5	0.877	99.7	5.45	287.4	0.776
VI		143.3	6.34	5.0	0.882	76.2	8.22	319.3	0.899
VII		153.0	6.31	4.9	0.899	69.1	6.49	320.4	0.862
I	7	151.3	4.64	2.0	0.862	169.4	5.09	134.7	0.872
II		149.8	4.68	2.9	0.848	153.5	4.31	210.7	0.790
III		153.7	4.46	2.4	0.858	176.5	5.43	148.6	0.844
IV		171.4	4.42	3.5	0.848	152.4	6.54	258.9	0.861
V		77.6	4.44	2.9	0.851	150.6	4.34	198.8	0.794
VI		160.5	3.93	3.0	0.810	151.2	4.42	301.1	0.827
VII		180.3	4.70	3.3	0.862	159.6	6.71	303.3	0.889
I	12	63.6	4.35	1.2	0.912	98.6	9.63	200.5	0.847
II		37.4	3.72	2.5	0.891	94.1	7.44	250.4	0.838
III		72.0	4.00	1.7	0.905	92.5	5.66	196.8	0.840
IV		39.3	3.02	2.5	0.840	98.6	5.36	260.7	0.855
V		52.5	3.31	2.3	0.885	115.5	8.50	216.6	0.858
VI		66.3	3.82	2.5	0.916	95.5	6.03	240.2	0.865
VII		42.6	3.74	2.5	0.913	97.5	5.35	270.3	0.856

dissolution with increase in pH [23]. Increase in dissolution is probably aided by increase in porosity, which suggests that barrier films of lower protective capabilities are formed in the solutions with higher pH, indicating the intervention of the hydroxyl anion. Furthermore, dissolved oxygen in the forming medium plays a significant role in improving the passive behaviour of the surface film on the steels.

The influential role of molybdenum as an active partner in forming a more stable passive film on the steel surface with good anticorrosive properties can be readily perceived by comparing R_T values for steels I and III which differ only from each other in their Mo content (0.3 and 3.0 wt%, respectively). The present results indicate that Mo addition enhances the resistivity of the film, increasing the R_T value, which is more pronounced in neutral and alkaline solutions. On the other hand, in oxygenated acidic buffer solutions (pH 2) steel I surpasses steel III in its R_T value. This may be due to the difference in the solubility limit of the chromium-rich salt layer [24].

EIS measurements were also conducted for steel III after 3 h immersion in neutral sulphate and chloride solutions. Over the concentration range studied (0.025 M–1.0 M) the simulated response of the representative circuit shown in Figure 8(c) compares well with the experimental results both in admittance and impedance planes. Figure 9 describes the variation of the frequency-independent total resistance (R_T) of the electrode impedance as a function of solution composition in sulphate and chloride media. It is well established that the properties of stainless steel favour the spontaneous formation of an oxide passive film which confers great resistance to corrosion in aqueous solutions. For a certain level of Mo in the steel, Figure 9 shows that in neutral sulphate solutions the R_T parameter of steel III decreases steeply at first and then slowly with increasing Na_2SO_4 concentration, perhaps through the reduction in the thickness of the surface passive film due to its excessive dissolution. The mode of variation of R_T in sulphate media indicates that equilibrium tends to be established at relatively higher concentrations (>0.5 M). On the other hand, in NaCl solutions the passive properties of the same steel are different where the R_T value decreases continuously with increasing NaCl concentration up to ~ 0.5 M, then starts to increase significantly to higher values as the Cl^- ion concentration increases.

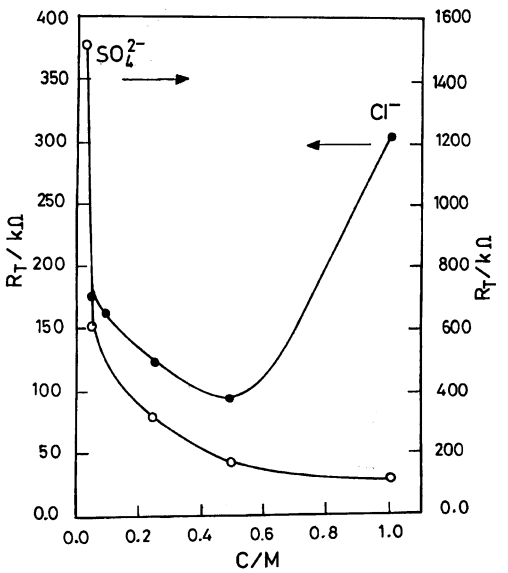

Fig. 9. Variation of the R_T value for steel III with the molar concentration (C) of Na_2SO_4 and NaCl solutions.

It seems that Cl^- can participate in enhancing the formation of soluble oxochlorocomplexes encompassing Mo [20] which initiate pit nucleation at the active inclusion sites leading to an increase in corrosion rate or R_T decrease. Increasing the Cl^- ion concentration (> 0.5 M) greatly reduces the solubility of these species. A possible concomitant hydrolysis reaction also cannot be excluded. This generates insoluble salts or hydroxides that hinder contact between the metallic surface and the electrolyte in the pit with a consequent decrease in the corrosion rate associated with increased R_T. The present results accord with those reported by Ougura et al. [25], who observed a threshold maximum corrosion rate at a concentration of ca. 0.2 M Cl^- for the alloys (18Cr–9Ni–0.01Cu-*x*Mo), *x* varied from 0.13 to 1.03 wt%.

Under open circuit conditions, it is suggested that the driving force for spontaneous surface oxide film formation on the metal is the free energy of the reaction between the metal and the solution. This reaction is assumed to proceed by migration of positive metal cations and/or oxygen vacancies of the metal towards the electrolyte, or possibly by migration of negative oxygen anions O^{2-} in the opposite direction [26]. It has been reported that the faradaic impedance due to metal dissolution at the oxide film/electrolyte interface depends strongly on the anion type, together with the local pH at the passive film [27]. In this respect, it has been shown [28–32] that Cl^- ions are incorporated in the passive layer when the passivation is performed in Cl^-containing electrolyte. Also, surface analysis results by Hubschmid et al. [33] showed that films grown in chloride containing sulphate solution incorporate the two electrolyte anions. In addition, the authors indicated that sulphate is located mostly in the outer part of the film with higher concentration (2–4 at%) than chloride (0.8–1.6 at%). All these support the results given in Table 4 and Figure 9 for steel III which show clearly that the R_T value in sulphate medium is much higher than in chloride. This behaviour suggests stabilization of the formed oxide film on the alloy surface due to incorporation of SO_4^{2-} ions in the oxide film during its growth to a much greater extent than in chloride medium. Anion incorporation in the oxide films greatly reduces their porosity [34, 35], leading to an increase in R_T.

4. Conclusions

Open circuit potential and EIS measurements carried out on seven Mo-containing stainless steels of various compositions reveal the following main points:

i) The open circuit potential (E_{oc}) transients all had similar trends, where E_{oc} changed positively until a steady state value (E_{ss}) was attained.

ii) The E_{ss} value increased with increasing Mo content in the alloy or decreasing solution pH, and decreased with O_2- removal from the test solution.

iii) Oxide film thickening followed a direct logarithmic growth law with two distinct rates δ_1 and δ_2 for the inner and the outer layers of the duplex passive films.

iv) For the same steel, E_{ss} was more positive in chloride than in sulphate solutions. In both cases, it varied linearly with the concentration according to: $E_{ss} = y - m \log C$.

v) EIS data showed that the total resistance R_T of the passive film for all tested steels tended to be lower in basic than in acidic buffer solutions, and acquired higher values in the oxygenated solutions.

vi) For a certain level of Mo in the steel, the R_T value of the passive film decreased steeply at first and then slowly with increasing SO_4^{2-} ion concentration. Also, increase in Cl^- ion concentration decreased the R_T value up to a critical concentration of ~0.5 M, then it started to increase again probably due to a reduction in the solubility limit of the film.

vii) R_T values in sulphate medium were much higher than in chloride, suggesting more stabilization for the formed passive film in the former solution as a result of the larger extent of SO_4^{2-} ion incorporation during growth.

Table 4. Equivalent circuit parameters for steel III in Na_2SO_4 and NaCl solutions of various concentrations

C/M	R_Ω/Ω	$Q/\mu F$	$R_T/k\Omega$	α
[Na_2SO_4]				
0.025	169.7	0.740	1512.0	0.794
0.05	102.2	2.660	613.1	0.811
0.25	24.8	3.878	318.9	0.807
0.50	161	6.956	169.4	0.799
1.0	12.4	7.125	109.2	0.814
[NaCl]				
0.05	144.6	2.084	176.1	0.776
0.10	67.5	4.436	163.2	0.852
0.25	32.6	4.830	124.5	0.792
0.50	24.1	3.700	94	0.721
1.0	16.6	2.259	308.2	0.843

References

1. M.J. Johnson, Bioprocess. Eng. Symp., (ASME, New York, USA, **53** 1988).
2. J.J. Parks, S.I. Pyum, W.J. Lee and H.P. Kim, *Corrosion* **55** (1999) 380.
3. C.O.A. Olsson and D. Landolt, *J. Electrochem. Soc.* **148** (2001) B438.
4. I. Betova, M. Bojinov, T. Laitinen, K. Mäkela, P. Pohjanne and T. Saario, *Corros. Sci.* **44** (2002) 2675, 2699.
5. K. Sugimoto and Y. Sawada, *Corros. Sci.* **17** (1977) 425.
6. H.H. Lee and H.H. Uhlig, *J. Electrochem. Soc.* **117** (1970) 18.
7. H. Ogawa, H. Omata, I. Itoh and H. Okdada, *Corrosion* **34** (1978) 52.
8. I. Olfjord and B.O. Elfstrom, *Corrosion* **38** (1982) 46.
9. J.M. Defranoux, *Materiaux et techniques* **62** (1974) 137.
10. R.F.A. Jargelius-Pettersson and B.G. Pound, *J. Electrochem. Soc.* **145** (1998) 1462.
11. Ju. Lurie, *Handbook of Analytical Chemistry*, English translation (Mir Publishers, 1975) 263.
12. A.M. Shams El-Din and N.J. Paul, *Thin Solid Films* **189** (1990) 205.
13. D.D. Macdonald and A. Sun, *Electrochim. Acta* **20** (2006) 1767.
14. M. Bojinov, G. Fabricius, T. Laitinen, K. Mäkela, T. Soario and G. Sundholm, *Electrochim. Acta* **46** (2001) 1339.
15. J.M. Abd El Kader and A.M. Shams El Din, *Br.Corros. J.* **14** (1979) 40.
16. I. Olefjord, B. Brox and U. Jelvestan, *J. Electrochem. Soc.* **132** (1985) 2854.
17. J.M. Abd El Kader, F.M. Abd El Wahab, A. El-Shayeb and M.G.A. Khedr, *Br. Corros. J.* **16** (1981) 111.
18. A.M. Shams El Din, L. Wang and T.M.H. Saber, *Br. Corros. J.* **29** (1994) 58.
19. F. El-Taib Heakal, N.A. El-Mobark, M.A. Ameer and A.A. Ghoneim, *Egypt. J.Chem.* **40** (1997) 281.
20. L. Wegrelius, F. Falkenberg and I. Olefjord, *J. Electrochem. Soc.* **146** (1999) 397.
21. Y.J. Kim, *Corrosion* **56** (2000) 389.
22. U. Rammelt and G. Reinhard, *Electrochim. Acta* **35** (1990) 1045.
23. B. Elsener and A. Rossi, *Mater. Sci. Forum* **192–194** (1995) 225.
24. J.R. Galvele, J.B. Lunsden and R.M. Staehle, *J. Electrochem. Soc.* **125** (1987) 1204.
25. S. Ogura, K. Sugimoto and Y. Sawada, *Corros. Sci.* **16** (1976) 323.
26. L. Young, *Anodic Oxide Films* (Academic Press, London and New York, 1961).
27. J.B. Bessone, D.R. Salinas, C.E. Mayer, M. Ebert and W.J. Lorenz, *Electrochim. Acta* **37** (1992) 2283.
28. S. Mischler, A. Vogel, H.J. Mathieu and D. Landolt, *Corros. Sci.* **32** (1991) 925.
29. C. Hubschmid and D. Landolt, *J. Electrochem. Soc.* **140** (1993) 1898.
30. W.P. Yang, D. Costa and P. Marcus, *J. Electrochem. Soc.* **141** (1994) 2669.
31. L. Wegrelius and I. Olefjord, *Mater. Sci. Forum* **185–188** (1995) 347.
32. S. Mischler, A. Vogel, H.J. Mathieu and D. Landolt, *Corros. Sci.* **32** (1991) 925.
33. C. Hubschmid, D. Landolt and H.J. Mathieu, *Fresenius J. Anal. Chem.* **353** (1995) 234.
34. G.T. Rogers, P.H.G. Draper and S.S. Wood, *Electrochim. Acta* **13** (1968) 251.
35. F. El-Taib Heakal, A.S. Mogoda, M.A. Ameer and A.A. Ghoneim, *Hung. J. Indus. chem. veszprém* **22** (1994) 29.